Published in final edited form as:
Neuroimage. 2010 January 15; 49(2): 1469–1478. doi:10.1016/j.neuroimage.2009.09.025.

Verification of fetal brain responses by coregistration of fetal ultrasound and fetal magnetoencephalography data

C. Micheli[1,2], **J. McCubbin**[3], **P. Murphy**[3], **H. Eswaran**[3], **C. L. Lowery**[3], **E. Ortiz**[2], and **H. Preissl**[2,3]

[1]Institute of Medical Psychology and Behavioral Neurobiology, University of Tübingen, Germany

[2]MEG-Center, University of Tübingen, Germany

[3]Department of Obstetrics and Gynecology, University of Arkansas for Medical Sciences, Little Rock, AR 72205, USA

Abstract

Fetal magnetoencephalography (fMEG) is used to study neurological functions of the developing fetus by measuring magnetic signals generated by electrical sources within the fetal brain. For this aim either auditory or visual stimuli are presented and evoked brain activity or spontaneous activity is measured at the sensor level. However a limiting factor of this approach is the low signal to noise ratio (SNR) of recorded signals. To overcome this limitation, advanced signal processing techniques such as spatial filters (e.g. beamformer) can be used to increase SNR. One crucial aspect of this technique is the forward model and, in general, a simple spherical head model is used. This head model is an integral part of a model search approach to analyze the data due to the lack of exact knowledge about the location of the fetal head. In the present report we overcome this limitation by a coregistration of volumetric ultrasound images with fMEG data. In a first step we validated the ultrasound to fMEG coregistration with a phantom and were able to show that the coregistration error is below 2 cm. In the second step we compared the results gained by the model search approach to the exact location of the fetal head determined on pregnant mothers by ultrasound. The results of this study clearly show that the results of the model search approach are in accordance with the location of the fetal head.

Introduction

The two emerging techniques for the study of fetal brain function *in utero* are functional magnetic resonance imaging (fMRI) and fetal magnetoencephalography (fMEG). Functional MRI provides both functional and anatomical information but has inherent limitations that include the difficulty in accessing the measuring space, high sound levels, and safety issues based on the exposure of the fetus to high magnetic fields and field gradients (Fulford et al., 2003 , Hykin et al., 1999, Moore et al., 2001, Jardri et al., 2008).

Fetal MEG is a completely passive and non-invasive methodology with superior temporal resolution developed for the recording of magnetic signals from the fetal brain. This technique has the potential to provide physicians with a non-invasive instrument capable of direct

NIH-PA Author Manuscript
NIH-PA Author Manuscript

neurological assessment of the fetus during pregnancy. Because fMEG does not provide anatomical imaging, this additional information must be obtained by complementary imaging techniques such as ultrasound (Eswaran et al., 2002, Gutierrez et al., 2005, Preissl et al., 2004).

Until recently, there have been no appropriate models for the generation of biomagnetic and electrical signals originating in the abdomen. This is because whole-abdomen recordings were impossible before fMEG, and also, no coregistered 3D ultrasound (US) imaging technique was available. To illustrate the importance of an appropriate model, one can consider the equivalent conducting sphere approach for the adult MEG recordings. In this field, 3D MRI recordings are used to generate a conducting sphere model of the head. This model allows location of the generating source of a measured signal with high precision.

For fMEG, this issue has been approached by describing the conductive properties of the fetal brain as a sphere inside the mother's uterine volume (Vrba et al., 2004b). A conductive sphere is used for modelling the secondary currents according to the forward solution introduced by Sarvas (1987) and is necessary to identify the locations and time courses of current generators for sensor-recorded activity (inverse problem). Based on the lack of an exact model for fMEG a technique, called 'model search' was developed (Vrba et al., 2004b, McCubbin et al., 2007). Model Search uses a linearly constrained minimum variance (LCMV) beamformer analysis (Van Veen et al., 1997) which systematically varies the location of the spherical conductor inside the maternal abdomen as well as a dipole source within the sphere, and determines the best fitting models. For identification of the best models, a statistical test on the reconstructed evoked response time course was used. Until now, the results of this technique have not been verified by anatomical superimposition. The ambiguity of the model search solution limits the localization accuracy to about one fetal head diameter, determined by the low signal to noise ratio for fMEG (Vrba et al., 2007).

Additional anatomical information with high spatial resolution can be gained by magnetic resonance imaging (MRI). However this technique is not routinely used in healthy fetuses. Moreover, the position of the mother in the MRI scanner is completely different as compared to her position on the fMEG system and would cause an unpredictable displacement of the internal anatomical structures of interest. We therefore chose to use ultrasonographic imaging. Ultrasonography provides images which, from the point of view of spatial resolution, already allow us to locate the conductor model (fetus' head) inside the volume of the maternal abdomen. The solution of the magnetic inverse problem finally allows us to identify the brain activity sources by means of a model search.

We performed two studies in order to develop, validate and apply the coregistration procedure between 3D ultrasound and fMEG. In the first study a phantom is used to determine the reliability of the coregistration without the added complexity of fetal movement. Based on the results we performed a second study with pregnant subjects to show that the anatomical information obtained by 3D ultrasound is in accordance with the solution of our model search approach.

In the Materials and Methods section, we explain: (1) how the coregistration procedure has been set up on the ultrasound/magnetic phantom, and (2) how we determine the anatomical and functional head models, when measurements are recorded from pregnant subjects in a clinical environment.

In the Results section we show the reliability of the coregistration on a phantom and we use the maximum localization error to define the error limits for the pregnant subject studies. We also present the results of the extraction of the anatomically based conductive sphere from the subjects' ultrasound images. We report radii of the fitted conductive spheres and their locations in the abdominal compartment. Finally we compare this anatomical information with beamformer model search results. In the Discussion and Conclusions section a summary of the results is presented and limitations in the implementation are discussed.

Materials and methods

The experiments were carried out at UAMS (University of Arkansas for Medical Sciences, Little Rock, AR) in the SARA lab (Preissl et al., 2004). SARA is an acronym for SQUID Array for Reproductive Assessment (CTF Systems Inc., Port Coquitlam, BC, Canada), and is the first MEG device specifically dedicated to recordings on pregnant women (see figure 1.a). The system is installed inside a magnetically shielded room (MSR) to reduce external magnetic interference.

The setup for the coregistration (figure 2) consists of the SARA device, fMEG reference coils, a system of magnetic sensors (Flock of Birds, FOB, Ascension Technology Corporation, Burlington, VT), a US system (Voluson 730 expert, GE Medical Systems), an acquisition PC, a custom made phantom, and pregnant subjects. The ultrasound transducer used for our experiments is a convex B-mode probe.

Fetal MEG reference coils detect the exact positions in 3D space (on phantom or subjects) in relation to the MEG sensors. The coils are attached to the maternal abdomen at three positions all approximately in the same plane: maternal left, right and middle of back. A fourth coil is then placed on the anterior abdomen at the site of the fetal head as detected by ultrasound imaging (Fig 1.c, 1.d).

The FOB system is a tracking system which records the position of three sensors (placed on the maternal abdomen in the exact same positions as the fMEG coils) which acquire the signal of a magnetic field transmitter and convert it in spatial coordinates relative to its center. This equipment is necessary to identify the reference points of the maternal abdomen in an absolute or a relative coordinate space and to determine the orientation of the ultrasound slices relative to a real world coordinate system.

The process of ultrasound volume reconstruction with the aim of coregistration of the anatomy and brain signals requires knowing the orientation of the slices relative to a reference system. Unlike an MRI coregistration technique for adult MEG, the field of view of US is limited by the depth of the ultrasonic wave. It is therefore impossible to image the fiducials simultaneously. In order to know the world coordinate of the slices, we use a tracking system and coordinate referencing software (3D Freescan 5.0, EchoTech 3D Imaging Systems GmbH, Hallbergmoos, Germany) in conjunction with a FOB sensor mounted on the US transducer probe. During the US scanning, the images are stored on a PC with orientation and position information of the US probe in relation to the three reference coils. This allows us to determine the voxel coordinates of the US slices in the coordinate system determined by the three reference coils.

Phantom experiment

As depicted in figure 2, the phantom is filled with water and an ultrasound sweep is run with a convex probe. The phantom consists of a Plexiglas container with a thin sponge material floor to prevent US reflections. A plastic cylinder sits inside with a plastic screw fixed to its surface. The aim of the sweep is to visualize clearly the plastic cylinder with its screw.

A scheme of the post processing is shown in figure 3. The coordinates and orientation of the sensor attached to the ultrasound probe are used to re-slice the free-hand ultrasound images and the software then reconstructs the imaged volume. Each voxel of the reconstructed set of slices is automatically referred to the origin of the system of reference, corresponding to the position of the transmitter.

The experimental coregistration error in the phantom is determined by a three step procedure: (i) storage of MEG reference coils coordinates in the fMEG datasets by means of standard localization procedure, (ii) ultrasound free hand sweep collection and FOB coordinate storage, and (iii) mathematical processing of the collected coordinates to estimate the US to fMEG roto-translational matrixes (coregistration).

The phantom and its support (a wooden board, see center box in figure 4 and positioning scheme in figure 5) are placed near SARA to collect the positions of three references (Back, Left and Right) plus one 4th coil taped on a plastic screw, taken as a reference visible in the US images. Reference coordinates are determined by a localization feature of the CTF MEG System which localizes the reference coils in space by selective activation of the coils at particular frequencies and determination of their positions in the 3D space of SARA dewar coordinates. Later the Plexiglas container is filled with water and US images are collected, along with reference positions, by means of the FOB tracking system.

Placement of the three FOB references must correspond to the SARA references, but since the dimensions of the sensors are different they do not match precisely. To correct for the mismatch, an offset in the z-axis is introduced for the FOB reference coordinates so that the nominal centers are aligned. This quantity takes into account the nominal values of MEG coils and FOB sensors heights (respectively 5 and 20.3 mm) given by technical specifications (Ascension guide, 1994), and the offset was defined as half of their difference.

The coregistration error is calculated as the root mean square (rms) error between the coordinates of the US references expressed in head coordinates and the SARA references in head coordinates.

$$co\_err=\sqrt{(Sara_{Back}-FOB_{Back})^2+\left(Sara_{Left}-FOB_{Left}\right)^2+\left(Sara_{Right}-FOB_{Right}\right)^2} \tag{1}$$

To express the FOB references in head coordinates according to the CTF axis convention a transformation matrix must be applied to their values in the original FOB domain.

According to CTF documentation the origin is located in the middle point between Left and Right coils and the x axis has the direction from the origin which points to the Back (Fig 2, upper right box).

At a 90° angle on the plane of Left and Right the y axis from the origin points out in the direction of the Left coil, without necessarily intersecting it. The z axis is perpendicular to both.

The x, y, and z unit vectors are calculated as follows:

$$\mathbf{origin}=\frac{\mathbf{Left}+\mathbf{Right}}{2} \tag{2}$$

$$\widehat{\mathbf{x}}=\frac{\mathbf{Back}-\mathbf{origin}}{\|\mathbf{Back}-\mathbf{origin}\|}\quad \widehat{\mathbf{z}}=\frac{\widehat{\mathbf{x}}\times(\mathbf{Left}-\mathbf{Right})}{\|\widehat{\mathbf{x}}\times(\mathbf{Left}-\mathbf{Right})\|}\quad \widehat{\mathbf{y}}=\widehat{\mathbf{z}}\times\widehat{\mathbf{x}} \tag{3}$$

where X is the vector cross product, ‖·‖ is the norm operator, the ^ indicates a unit vector quantity, and **Back**, **Left**, **Right** are respective coil position vectors.

Once the unit vectors are known the rotation matrix and the translation vectors are computed as:

$$\mathbf{R}=\left(\frac{\begin{matrix}1 & 0 & 0\\ 0 & 1 & 0\\ 0 & 0 & 1\end{matrix}}{\begin{matrix}\widehat{x}_x & \widehat{y}_x & \widehat{z}_x\\ \widehat{x}_y & \widehat{y}_y & \widehat{z}_y\\ \widehat{x}_z & \widehat{y}_z & \widehat{z}_z\end{matrix}}\right)^{-1},\ \mathbf{T}=-\,\mathbf{origin} \tag{4}$$

These are the transformations applied to a point in SARA dewar coordinates or in FOB world coordinates, in order to coregister in head coordinates according to CTF conventions.

The rms differences between FOB and SARA coil distances indicate how much the two triangles described by the reference coils in the different modalities are displaced and gives therefore an assessment index for the coregistration procedure.

Finally we determine the mismatch between the localization of SARA's 4th coil and screw tip in the ultrasound images. This measure is not essential for the coregistration assessment but provides additional information about the quality of the coregistration procedure.

The localization mismatch is quantified by the mean distance between the SARA 4th coil and US points for every position of the phantom, as:

$$d_K=\frac{1}{n}\sum_{i=1}^{n}\sqrt{(P_{i-us}-4th_{Sara})^2} \tag{5}$$

where P_{i-us} is the US coregistered point corresponding to the screw tip, $4th_{Sara}$ is the corresponding SARA 4th coil in head coordinates and n is the number of measures in a particular position of the phantom (K=A,B,C,D see figure 2).

For the localization of points in the US space we use the 3D reconstruction of the collected sweep and visualized the volume in Matlab (MathWorks Inc., Natick, MA) with a volumetric graphic tool. The coordinates of the screw are determined through manual marking of the tip (figure 4, right) and the transformation voxel to FOB world coordinates is defined in the Echotech software as

$$\mathbf{Xscs}=\mathbf{R}(\mathbf{Svtmm}\cdot\mathbf{Xvcs}+\mathbf{T}) \tag{6}$$

where **Xvcs** is the point in voxel coordination system, **Xscs** is the point in FOB sensors coordination system (in mm), **Svtmm** is the voxel to millimeters scaling matrix, **T** is the translation vector and **R** is the orientation matrix.

For the coregistration we have to estimate the rotation matrix and the translation vector which allow the three points of FOB references to be transformed to the corresponding points in the fMEG space. The rotational and translational matrixes are estimated with a rigid body roto-translation algorithm.

The coregistration error is the rms localization difference between FOB references and fMEG references after coregistration to a common nominal reference system defined by CTF head coordinates (see eq. (1)).

Once the rotational matrix **R** and the translation vector **T** are known, the coordinates of each of the voxels in the US image in fMEG space coordinates can be determined by the following equation:

$$\mathbf{P'us} = \mathbf{R} \cdot \mathbf{Pus} + \mathbf{T} \tag{7}$$

Study with pregnant subjects

Measurements were performed on 18 healthy subjects with normal pregnancies who gave written consent according to UAMS Human Research Advisory Committee regulations.

The study is divided into two parts, the first refers to the US collection, and the second is a standard fMEG protocol. The standard fMEG recording is divided in three different sessions consisting of an auditory stimulation, spontaneous activity recording and a visual stimulation (10 minutes each) as described in Preissl (2004).

The US collections were performed using a mock-up model of the SARA system (described in figure 1) in order to minimize subject repositioning mismatch between the US and the fMEG session. This mock-up system is configured so that the subject's body position during the US measurement is identical to her body position during the fMEG study.

During the first part of the study, three FOB sensors are positioned on the maternal abdomen in the Left, Right and Back position according to SARA conventions (CTF documentation). These points are marked on the skin and sensors are kept in place with suitable surgical adhesive tape. In the second part, the FOB sensors are removed and the fMEG reference coils are positioned onto the marked locations and the fourth coil is positioned in the abdominal quadrant containing the head, after inspection with US and just before running the standard fMEG protocol.

The outcome of the study consists of (a) the fitting parameters of the fetal head model (center and radius) obtained after marking the fetal head shape on the US slices and coregistration of the marked points and (b) the fMEG data. The assumptions made on the basis of phantom coregistration define the acceptance criteria to evaluate the coregistration quality.

A beamformer model search applied to fMEG data provides a sphere (obtained with the model search algorithm), which can confirm independently the results of coregistration.

The beamformer model search was performed on each of the two data segments of auditory or visual stimulation for subjects with a coregistration error smaller than 2 cm. A priori information that was required for the model search included the choice of an electromagnetic model (dipole in a conducting sphere), fetal biometrics estimated from the US exam (head diameter, head to heart distance, head to maternal abdomen distance, and fetal orientation within the maternal abdomen), and fetal heart location estimate. These are all objective measures applied uniformly across the individual data collection sessions.

Prior to the model search the fetal heart location was estimated from an initial beamformer model search over the maternal abdominal volume using fetal QRS signals. This location in combination with US information concerning head-heart distance was used to construct a search grid (1 cm spacing) for the evoked response model search. The head diameter was standardized at 10 cm for the model search since there was only small variation among the subjects.

The beamformer implementation was modified from that described in McCubbin et al. (2007) to identify sphere models corresponding to significant clustered source activity (Frey and Dueck, 2007). In order to identify the location in the 3D space corresponding to significant time course activity after trigger presentation, a z-statistic was computed including a noise estimate derived by surrogate testing. Cluster analysis was applied on the voxels with z values larger than 2 according to statistical flattening as described in Barnes and Hillebrand (2003) and the clusters which passed the test for significance were selected. Their corresponding head models were then used for comparison with the anatomical model. A detailed description of beamformer model search is beyond the scope of this report and **is** described in a separate publication (McCubbin et al., 2009).

Results

Phantom coregistration

We report the output of the coregistration procedure collected on the Plexiglas phantom and relative to several ultrasound sweeps coregistered to a particular fMEG reference coil configuration (see table 1). In the table the configuration with the highest coregistration error is represented.

We consider an experimental set-up in which the phantom was placed in four different orientations (denoted by indexes A to D, see first column in table 1). The number of repetitions for each session is reported in column 2 and refers to the number of sweeps run according to the scheme of figure 2. Each configuration (A to D) refers to the same position of the three reference coils (Left, Right and Back) previously localized in the fMEG.

The quality of coregistration is calculated by means of two indexes: rms error (column 3 and 4) and distance between 4th coil-coregistered and the tip of the screw (columns 5 and 6). Figure 6 presents the US marked points in the fMEG sensors space.

According to these results the maximum rms error of coregistration varies approximately around 20 mm and depends exclusively on the acquisition of US and fMEG fiducials. It is reasonable to assume this value as an upper limit for the error in the coregistration procedure.

Construction of the sphere for the forward model

For the construction of the forward model, the simplest approach is a homogenous conducting sphere (Vrba et al. 2004b, 2007). For the extraction of the sphere from the US data, multiple points on the reconstructed US images are marked to determine the fetal head diameter and the center of the sphere. After marking (see scheme in figure 3), each point is coregistered to fMEG dewar coordinates and a single sphere is fitted to these points (see the example of figure 7).

The algorithm processes the selected points with an unconstrained minimization fit so that they are all equally distant from a calculated center (function ‘fminunc’ implemented in the Matlab Optimization toolbox).

Figure 8 shows the fitted head center in the fMEG sensors space along with the positions of the reference coils, which delimit the maternal abdomen.

As a result, the parameters of the fitted spheres are reported in table 2 for all the subjects. The dewar coordinates of model centers are shown in column 3 (mm) along with model diameters (column 4).

Abdominal coregistration

In table 3 we present the coregistration errors for all the subjects and the distances between 4^{th} coil and transducer probe. One subject was excluded from the study because of interrupted collection of fMEG data.

Nine subjects out of the 17 passed the error criterion (table 3) and were further analyzed (source identification). Subject 10 was excluded because of the high mismatch in the 4^{th} coil-transducer distance.

Model search results

For the evoked response model search we used a 10% false positive rate. The ten minute recordings were separated in 2 minute time slices with an overlap of 1 minute, resulting in nine segments. Each of the time slices was used for model search and significant activation was recorded. In seven out of nine datasets, statistically significant averaged activity was found in at least one of the segments. All significant model search origins were found to be within one fetal head diameter of the US model, as expected for source ambiguity in a low SNR application (Vrba et al. 2007). An example of the model search analysis is given in figure 9, which represents a typical result of the beamformer. Gray circles show the spherical models with significant cluster sources along with the coregistered ultrasound model (black thick circle). All of them are within one head diameter distance from the coregistered model.

Discussion and conclusions

We have shown with phantom experiments that it is possible to coregister a 3D US image with fMEG. The inherent error of the procedure is about 2 cm. Primary sources of error included FOB measurement accuracy and manual image marking. However the manual error for the marking of the screw tip is around 5mm (based on the size of the screw tip). For the sphere center we estimated an error of 3.5 mm. The first measure has been determined from the maximum number of slices in which the screw center is visible by checking the presence of a point (a clay snippet has been applied) in the upper part of the screw which is maximally contrasted (see fig.10 a–b), The sphere center error has been calculated by running the manual localization procedure 10 times (see fig.11) on subject 1. We selected ~150 points at each run by looking at the most contrasted voxels at the head rim and taking care that at the end the curvature of the head was represented. Out of these, 10 spheres have been fitted and the correspondent centers have been plotted. Consequently we calculated standard deviation of centers and took 4 times this value as the error (95% probability assuming the cloud of points around the mean to be normally distributed).

Based on this result we were able to apply the coregistration procedure for fMEG measurements, in which we obtained coregistered anatomical information. The beamformer results with a successful coregistration show that statistical source analysis is able to detect significant activations in the vicinity of the coregistered fetal head location.

In fact, on the basis of ultrasound 3D image reconstruction and coregistration in the fMEG space, the correspondence between ultrasound model and model search is in agreement with the ambiguity region (approximately one head diameter) for beamformer analysis with low SNR (Vrba et al., 2007). This result suggests that it is appropriate to use a model search to detect fetal brain activity in an evoked response protocol and this activity is generated in an abdominal space which is in accordance with the fetal head. On this basis we can reasonably assume that the localized sources are generated by brain activation in response to repetitive auditory or visual stimuli.

The coregistration procedure included fMEG fiducials localization, FOB localization, data transfer to the processing computer, and post processing. The whole procedure took altogether around 10 minutes. US pictures collection, data transfer and sphere fitting took another 20 minutes. fMEG recordings were conducted for 30 minutes and the beamformer model search took around 120 minutes. Altogether, the whole procedure lasted around three hours for a single subject.

It is not always possible to get an ideal coregistration, especially if the ultrasound measurements are performed outside of the MSR. Coregistration performance can be dependent on unpredictable factors such as displacement of the reference coils, maternal movements due to respiration or general maternal movements during acquisition, skewed positioning in the mock-up with respect to the SARA system, deformability or lateral displacement of the maternal abdomen, and further unknown circumstances. These factors, which cannot be determined for the single subject, can result in a coregistration error exceeding the threshold of 2 cm in the excluded subjects.

For this reason, it is important to quantify a measure of reliability for the procedure that takes into account CTF relative abdominal coordinates to which ultrasound and fMEG absolute coordinate systems can be referred (coregistration error).

On the other hand, we must consider that the fetal head model is a static model relative to a position in the uterus at some time before the fMEG session. However, because the fetus may move before the fMEG recording is completed, an additional US examination is performed at the end of the fMEG collection to verify that the distance from the fetal head to the maternal abdomen remains unchanged. Subject 10 was excluded from further analysis because her measurements presented a big mismatch of the parameters collected at the beginning of the US analysis and at the end of the fMEG study. We hypothesize this to be due to fetal head displacement. However in all the other cases we have verified that once pregnant subjects are correctly positioned in both mock-up and SARA systems and the coregistration error is low; the model search is able to extract brain activity which is localized near the US fetal head model.

Suggested improvements for ultrasound coregistration include a better positioning of the mother in the experimental environment, i.e. a more stable seat with a more ergonomic shape, a continuous abdominal position tracking system to detect when movement exceeds a pre-determined threshold, and the capability to collect US sequences inside the MSR. The first enhancement has already been implemented in a new fMEG system, SARA 2, installed in the MEG Center of Tübingen. It is equipped with a highly ergonomic seating position which allows a longer duration of data collection with less maternal movement.

The implementation of the ultrasound coregistration procedure in a clinical setting is limited by the high exclusion rate and the inherently difficult and time consuming procedure. Nevertheless, the beamformer source reconstruction and cluster based statistics are a validated approach to extract time courses of evoked fetal brain activity, as recently reported in McCubbin et al. (2009). In conclusion, ultrasound co-registration in combination with a beamformer model suggest that the reconstructed sources may have been generated by fetal brain activity. Efforts are to be made to enhance signal-to-noise ratio in order to confirm these results.

Acknowledgments

This study was supported by NIBIB-National Institutes of Health grant R01EB007826-01A1.

References

Ascension. The Flock of Birds Installation and Operation Guide. Vol. 05402. Vermont: Ascension Technology Corporation POB 527 Burlington; 1994. p. 860-6440.

Barnes GR, Hillebrand A. Statistical flattening of MEG beamformer images. Hum. Brain Mapp 2003 Jan;18(1):1–12. [PubMed: 12454907]

CTF systems. Command Line Programs. manual number 900-0016-AW02 release 3.2.

CTF systems. Head Localization. :93–95. manual number 900-0017-AW02 release 3.2.

Eswaran H, Wilson J, Preissl H, Robinson S, Vrba J, Murphy P, Rose D, Lowery C. Magnetoencephalographic recordings of visual evoked brain activity in the human fetus. Lancet 2002 Sep 7;360(9335):779–780. [PubMed: 12241838]

Frey BJ, Dueck D. Clustering by passing messages between data points. Science 2007 Feb 16;315(5814): 972–976. Epub 2007 Jan 11. [PubMed: 17218491]

Fulford J, Vadeyar SH, Dodampahala SH, Moore RJ, Young P, Baker PN, James DK, Gowland PA. Fetal brain activity in response to a visual stimulus. Hum. Brain Mapp 2003 Dec;20(4):239–245. [PubMed: 14673807]

Gutierrez D, Nehorai A, Preissl H. Ellipsoidal head model for fetal magnetoencephalography: forward and inverse solutions. Physics in Medicine and Biology 2005;50(9):2141–2157. 2005. [PubMed: 15843742]

Hykin J, Moore R, Duncan K, Clare S, Baker P, Johnson I, Bowtell R, Mansfield P, Gowland P. Fetal brain activity demonstrated by functional magnetic resonance imaging. Lancet 1999 Aug 21;354 (9179):645–646. [PubMed: 10466668]

Jardri R, Pins D, Houfflin-Debarge V, Chaffiotte C, Rocourt N, Pruvo JP, Steinling M, Delion P, Thomas P. Fetal cortical activation to sound at 33 weeks of gestation: a functional MRI study. Neuroimage 2008 Aug 1;42(1):10–18. [PubMed: 18539048]

Leotta DF. An efficient calibration method for freehand 3-D ultrasound imaging systems. Ultrasound Med Biol 2004 Jul;30(7):999–1008. [PubMed: 15313332]

McCubbin J, Robinson SE, Cropp R, Moiseev A, Vrba J, Murphy P, Preissl H, Eswaran H. Optimal reduction of MCG in fetal MEG recordings. IEEE Trans. Biomed. Eng 2006;53:1720–1724. [PubMed: 16916111]

McCubbin J, Murphy P, Eswaran H, Preissl H, Yee T, Robinson SE, Vrba J. Validation of the flash-evoked response from fetal MEG. Phys Med Biol 2007 Oct 7;52(19):5803–5813. Epub 2007 Sep 10. [PubMed: 17881801]

McCubbin J, Vrba J, Murphy P, Temple J, Eswaran H, Lowery CL, Preissl H. Fetal MEG evoked response latency from beamformer with random field theory. Neuroimage accepted. DOI: 10.1016/ j.neuroimage.2009.08.019.

Milne AD, Chess DG, Johnson JA, King GJ. Accuracy of an electromagnetic tracking device: a study of the optimal range and metal interference. J Biomech 1996 Jun;29(6):791–793. [PubMed: 9147976]

Moore RJ, Vadeyar S, Fulford J, Tyler DJ, Gribben C, Baker PN, James D, Gowland PA. Antenatal determination of fetal brain activity in response to an acoustic stimulus using functional magnetic resonance imaging. Hum. Brain Mapp 2001 Feb;12(2):94–99. [PubMed: 11169873]

Pankratov, K. Matlab routine and comments for rigid body coregistration. www.mathtools.net/files/net/rotsolve.zip

Preissl H, et al. Fetal magnetoencephalography: current progress and trends. Experimental Neurology 2004;190:28–36.

Sarvas J. Basic mathematical and electromagnetic concepts of the biomagnetic inverse problem. Phys. Med. Biol 1987;32:11–22. [PubMed: 3823129]

Van Veen BD, van Drongelen W, Yuchtman M, Suzuki A. Localization of brain electrical activity via linearly constrained minimum variance spatial filtering. IEEE Trans Biomed Eng 1997 Sep;44(9): 867–880. [PubMed: 9282479]

Vrba J, Robinson SE, McCubbin J, Lowery CL, Eswaran H, Wilson JD, Murphy P, Preissl H. Fetal MEG redistribution by projection operators. IEEE Trans. Biomed. Eng 2004;51:1207–1218. [PubMed: 15248537]

Vrba J, Robinson SE, McCubbin J, Murphy P, Eswaran H, Wilson JD, Preissl H, Lowery CL. Human fetal brain imaging by magnetoencephalography: verification of fetal brain signals by comparison with fetal brain models. Neuroimage 2004 Mar;21(3):1009–1020. [PubMed: 15006668]

Vrba J, Robinson SE, McCubbin J, Lowery CL, Eswaran H, Murphy P, Preissl H. Searching for the best model: ambiguity of inverse solutions and application to fetal magnetoencephalography. Phys Med Biol 2007 Feb 7;52(3):757–776. Epub 2007 Jan 16. [PubMed: 17228119]

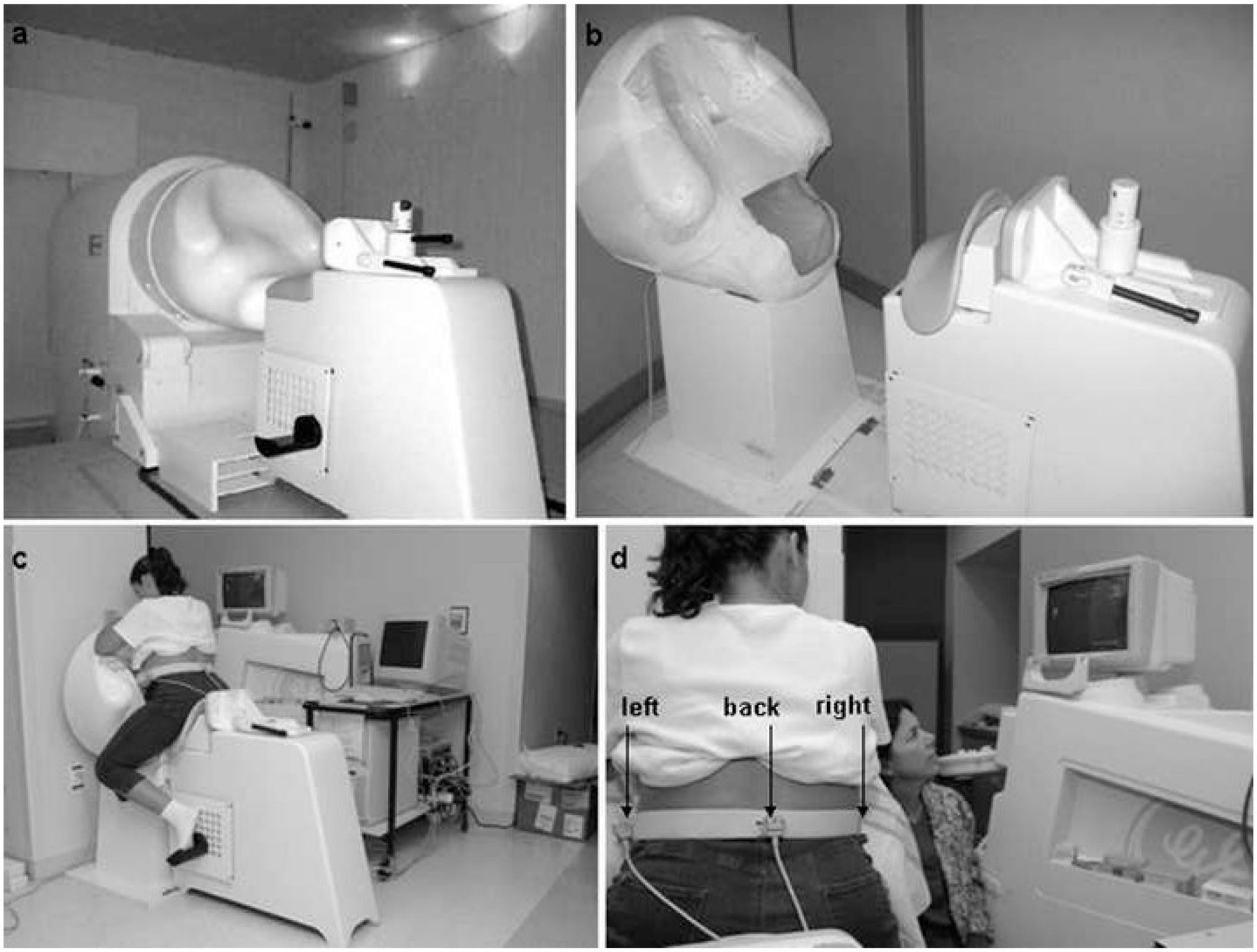

Figure 1.
The SARA system (a) and its mock-up model (b, c and d). The model has a carved aperture on its front side (b) so that mother's abdomen can be easily accessible for ultrasound measurements (c), (d). Reference coils positioned on abdominal fiducial points allow the coregistration of ultrasound images and fMEG activity (d).

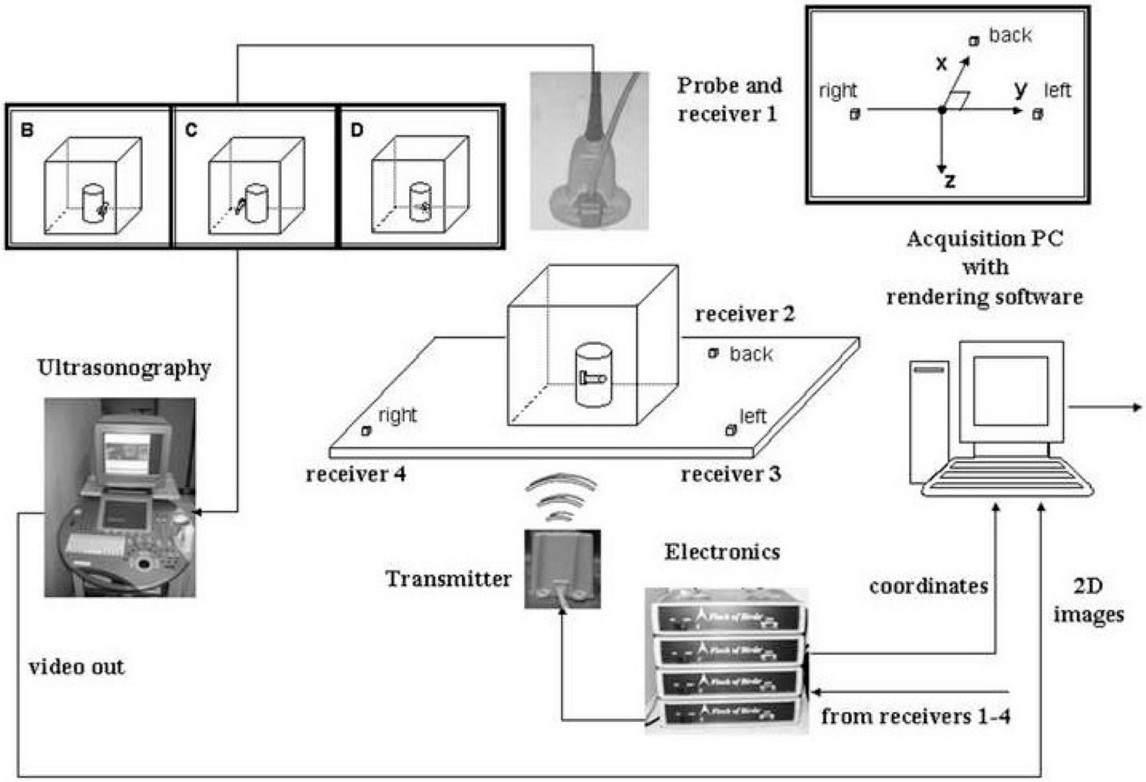

Figure 2.
Setup for the phantom acquisition. The phantom, in the middle, is filled with water and a sonographic sweep is run to collect the volume of the plastic cylinder inside it. A 3D image rendering is possible with reconstruction software and a magnetic tracking system (FOB) which transform the 2D sonographic images in a volumetric sequence of parallel slices. In the boxes (upper left) all the possible screw configurations are shown, starting from position A, as depicted in the center. A scheme of CTF MEG conventional coordinate system is shown herewith (upper right).

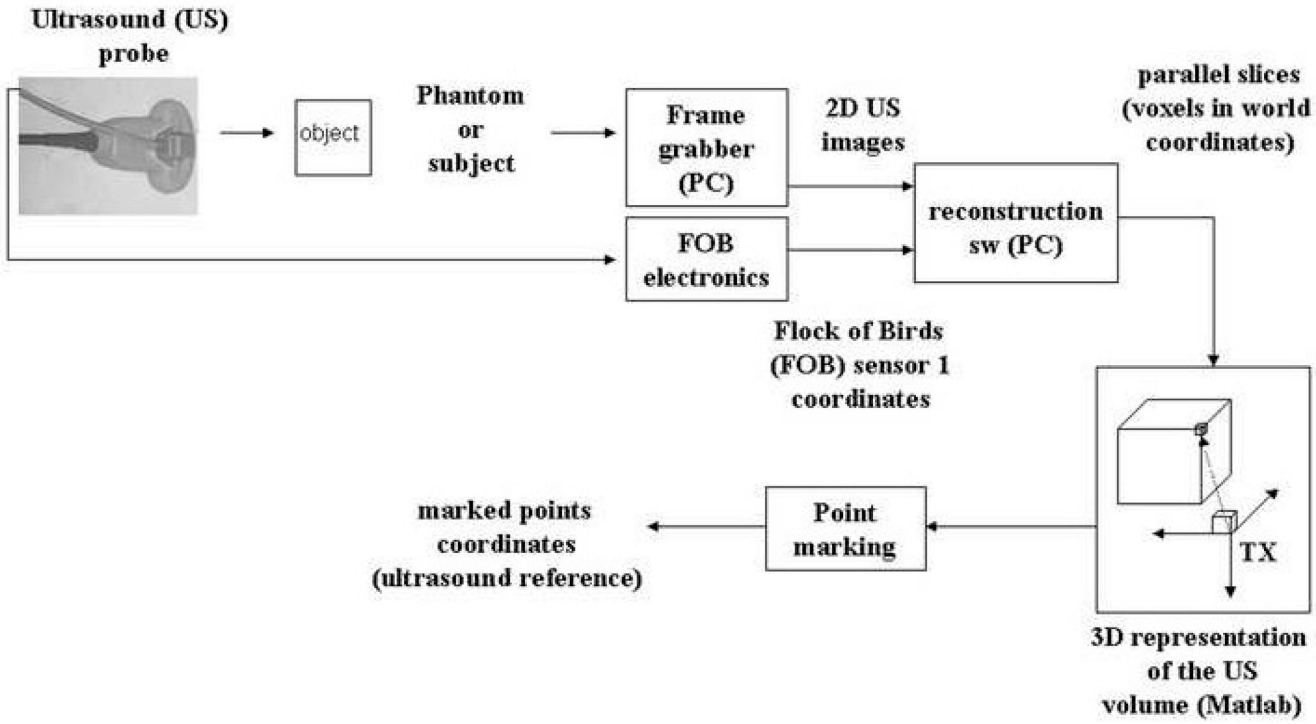

Figure 3.

Post processing flow chart to obtain the parallel slices of ultrasound volumetric images. The free-hand ultrasound sweep images are re-sliced by a reconstruction software and referred to the position of the transmitter.

NIH-PA Author Manuscript
NIH-PA Author Manuscript

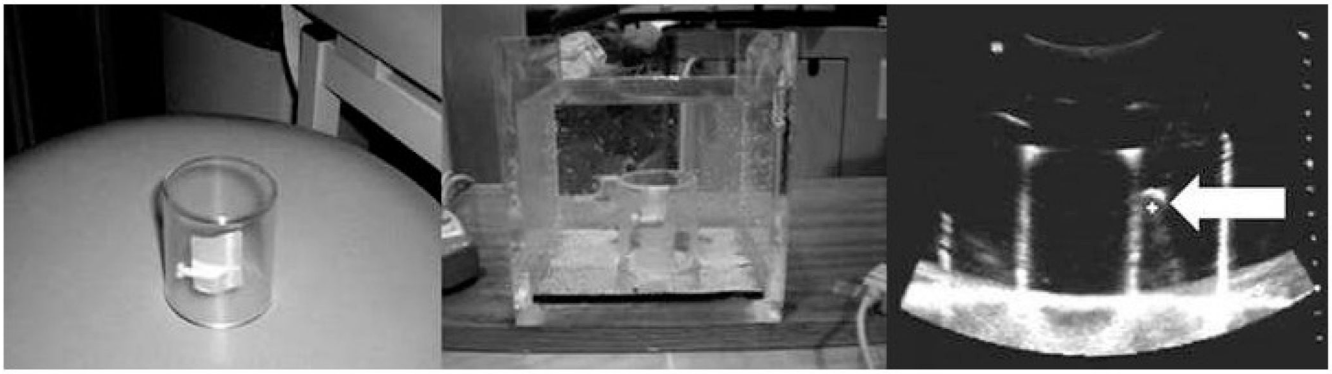

Figure 4.
A plastic cylinder shape (left) is used to localize a point in 3D space by means of phantom ultrasonography (center). The head of the screw (green arrow) is selected manually (red cross) after visualization with a software tool.

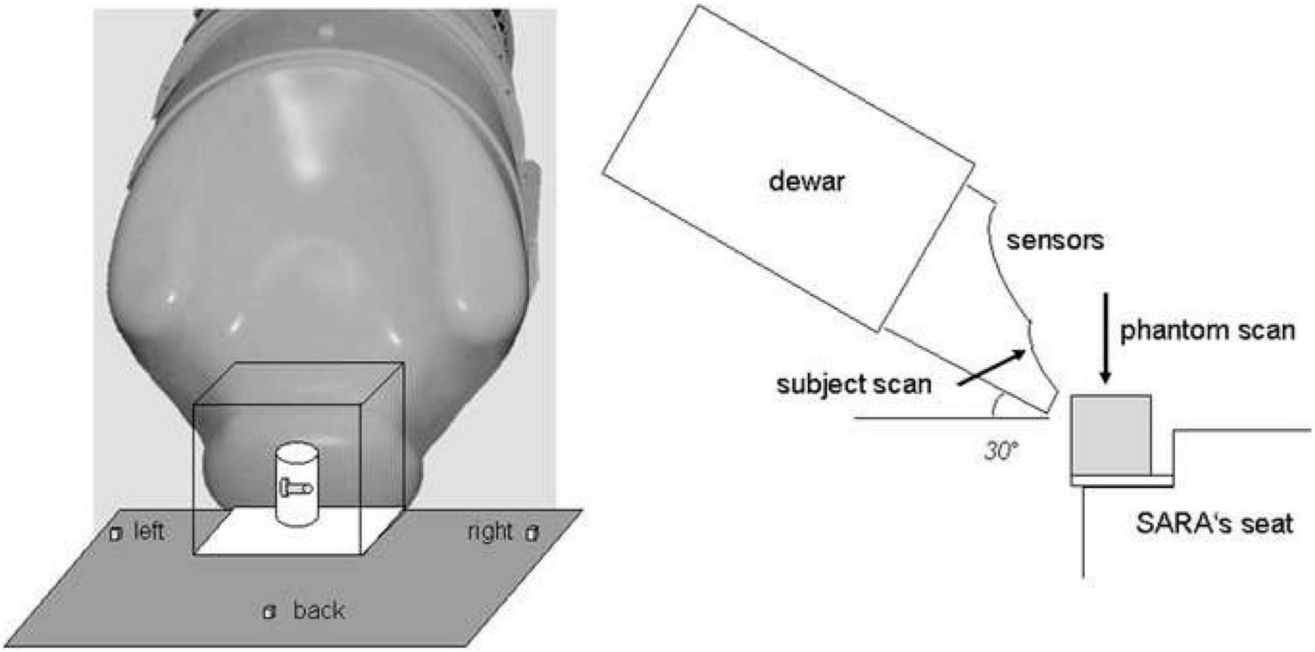

Figure 5.
A sketch of phantom position with respect to SARA (left). Phantom positioning seen from a lateral view (right).

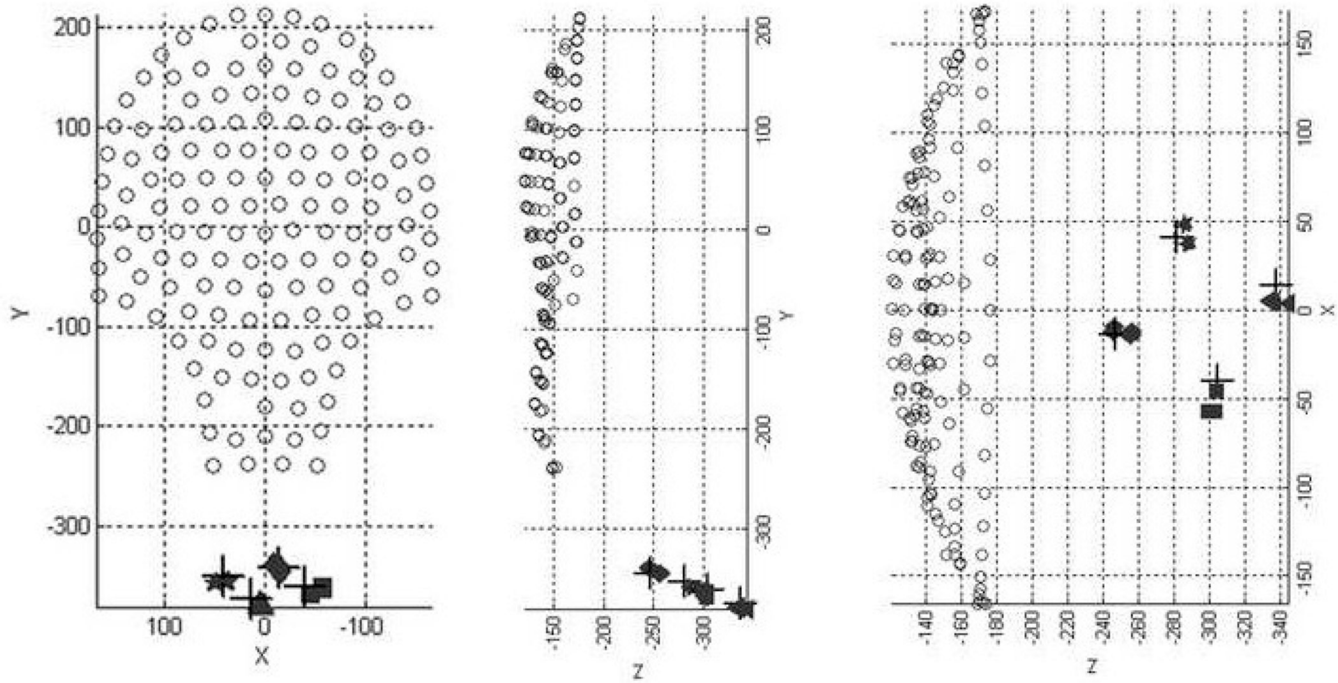

Figure 6.
Diamonds represent screw head points marked for position A, stars, squares and triangles indicate respectively position B, C and D. The black cross represents fMEG's 4th coil. All points are displayed in dewar reference system (30° tilted) and pick-up coils are depicted as unfilled circles.

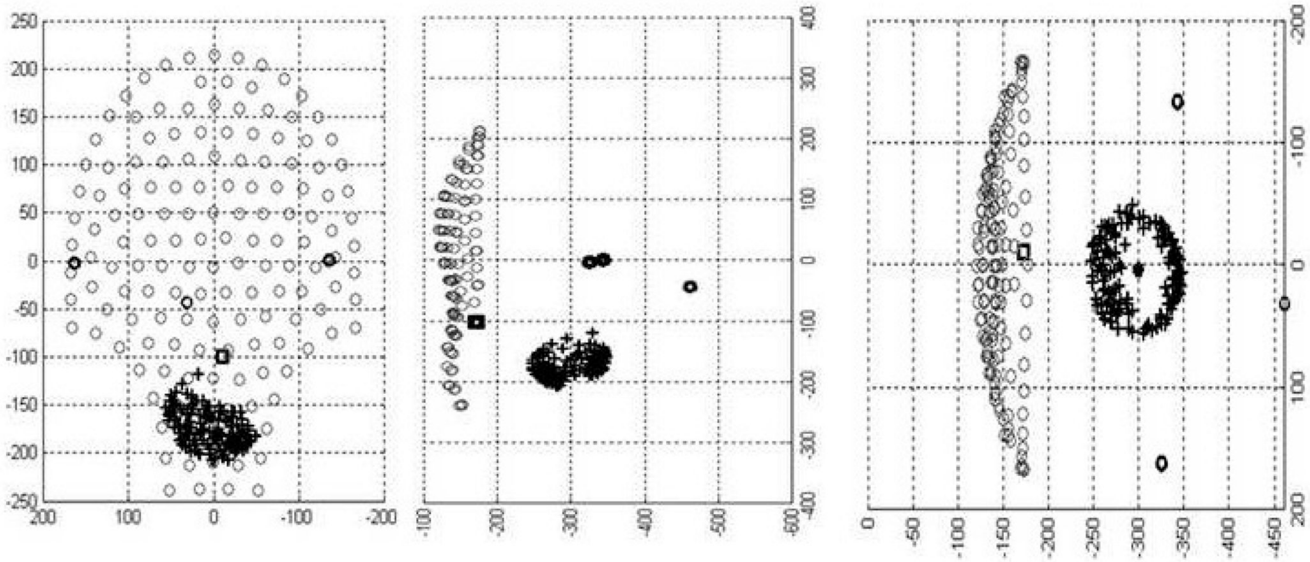

Figure 7.

Coregistered US points (crosses) relative to fetus' head shape, represented in fMEG dewar coordinates (subject 7). Thick unfilled circles represent Left, Right and Back reference coils on mother's belly. The square is the position of the 4th coil. The filled circle is the fitted sphere center.

NIH-PA Author Manuscript
NIH-PA Author Manuscript

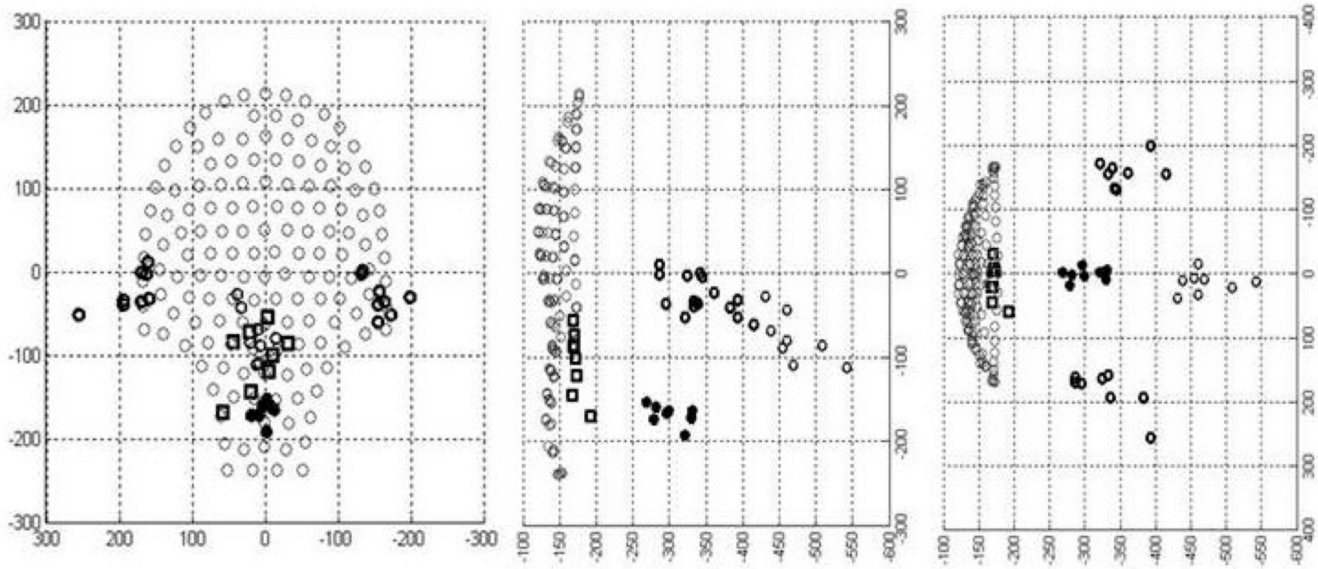

Figure 8.
fMEG reference coils for all subjects (unfilled thick circles for Left, Right and Back) and filled circles for fitted spheres' centers. The squares are positions of 4th coil.

NIH-PA Author Manuscript

NIH-PA Author Manuscript

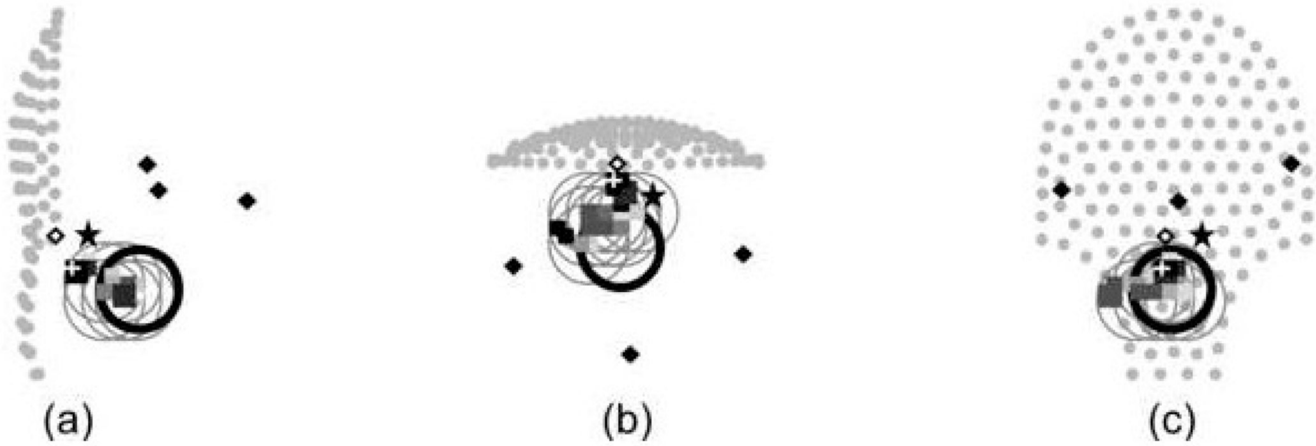

Figure 9.
Example of model search results for subject 16, projections onto (a) y–z, (b) x–z, and (c) x–y planes of: MEG sensor array (gray dots), abdominal coils (filled diamonds), 4th coil (unfilled diamond), fetal heart (star), US head model (thick black circle), all members of all clusters which passed statistical false positive threshold of 0.10 (gray scale squares, gray level is a function of source metric value with white as zero level so that sources with largest metric values are darkest. Overlaid with largest values on top), and associated models (gray circles), and finally one largest cluster center location (white cross).

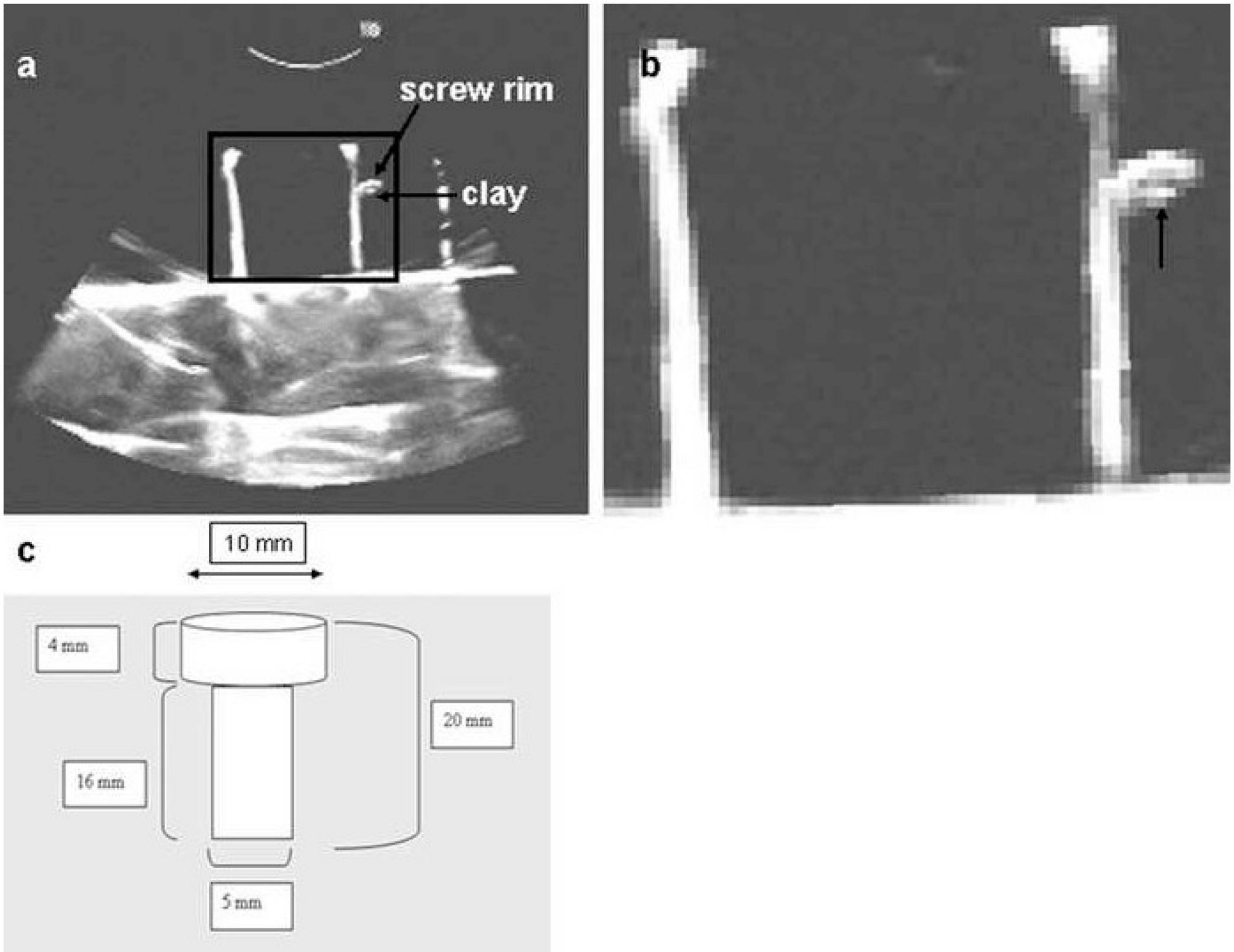

Figure 10.
(a) Phantom ultrasound 3D reconstructed slice. Arrows indicate a clay tip and screw rim (top left view). (b): Blow-up of the selected image box. The arrow points to the maximally contrasted voxel within the screw rim. (c): A sketch of screw geometry with dimensions in mm (side view).

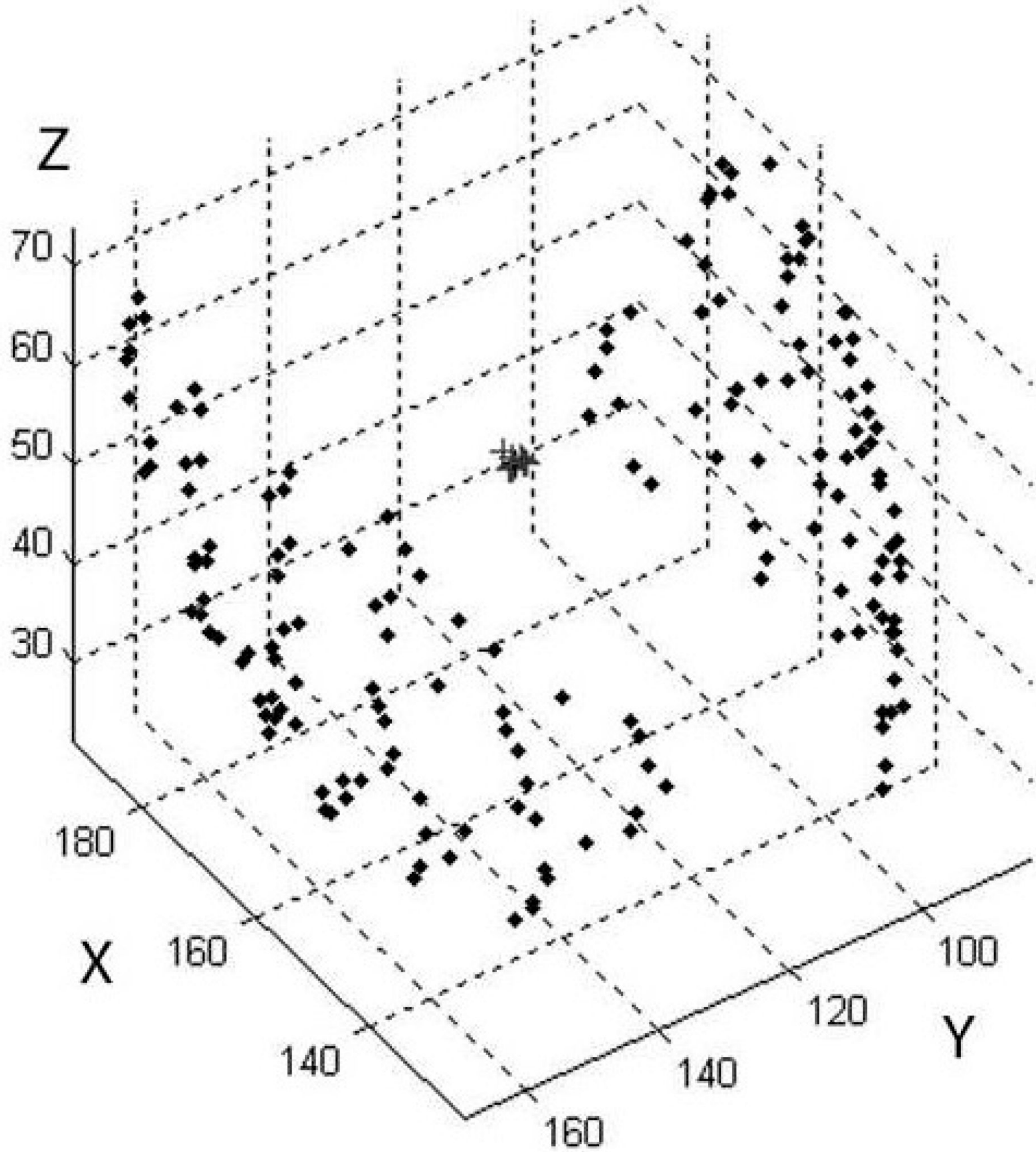

Figure 11.

A 3D scatter plot showing the manually selected points from abdominal US (dots, only one subject's dataset is marked), and a cloud of crosses indicating the sphere's center after fitting of ten different selections. An asterisk in the middle of the crosses cloud indicates the mean position of 10 centers. Units are in voxels.

NIH-PA Author Manuscript
NIH-PA Author Manuscript

Table 1

phantom coregistration error

Phantom coregistration error for every position (column 1: A, B, C or D). The mean and standard deviation (std) across different trials (column 2) are listed in columns 3 and 4. The 4^{th} coil distance from the coregistered screw tip point (d) mean and standard deviation across trials are listed in columns 5 and 6. All measurements are in millimetres.

dataset	recordings	mean(rms)	std	mean(d)	std(d)
posA	6	20.28	0.38	6.76	2.53
posB	6	20.65	0.24	10.19	1.53
posC	6	20.96	0.14	16.2	4.36
posD	6	20.8	0.19	12.39	1.81

Table 2

Fitted spheres' centers and diameters

Sphere centers (in dewar coordinates) and diameters of the corresponding model sphere for each subject is shown. The last two columns show the fitted ellipse's axes according to the US morphometries measured with GE Voluson tool. All values are in mm.

subject	Gestational Age (weeks-days)	Center (x y z)			diameter	US short axis	US long axis
1	34-4	−62	−14	−245	93	89	93
2	32-0	−104	17	8	87	85	89
3	33-2	18	18	147	91	89	104
4	32-0	−4	−15	94	88	84	105
5	30-4	30	−19	182	77	88	106
6	33-0	−32	−3	157	96	87	104
7	31-0	−25	15	130	88	79	102
8	31-6	12	10	149	92	88	106
9	33-3	−2	33	170	83	82	114
10	32-5	−15	−8	161	89	86	107
11	34-1	24	5	156	87	86	98
12	31-5	−61	−8	151	88	79	100
13	32-1	−39	−10	139	91	78	109
14	32-3	3	18	156	102	82	106
15	30-4	−110	−78	39	83	75	104
16	30-2	18	−22	138	85	77	100
17	32-1	−74	2	139	89	81	111

Table 3

Abdominal coregistration error

Abdominal coregistration error (rms of Back, Left, Right points) and distance of 4th coil to transducer probe detected on the US image and coregistered in fMEG domain. The dotted line indicates the coregistration error limit that was established in the phantom experiment.

subject	Coregistration error	d(4th-trans)	
2	8	21	
8	11	19	
11	14	16	
10	15	62	
1	16	12	
16	17	30	
4	17	29	
14	18	27	
13	19	16	
7	20	18	**20 mm**
6	28	40	
5	30	35	
17	35	25	
15	36	45	
9	38	41	
3	43	11	
12	46	46	